International Journal of Recent Technology and Engineering (IJRTE)
ISSN: 2277-3878 (Online), Volume-8 Issue-6, March 2020

Effect of Motion Artifact on Variation in Heart Rate Variability Parameters

Jae Mok Ahn, Jeom Keun Kim

Abstract*: The heart rate variability (HRV) is a noninvasive way properly for investigating the activity of the autonomic nervous system (ANS) as well as to predict cardiovascular diseases. To guarantee an accurate HRV analysis, a motion artifact-free HRV recording must be obtained. However, complete removal of a motion artifact is impossible when measuring heartbeats for 5 min, and the motion artifact due to sudden ANS activity must be taken into consideration for the HRV parameters. And, the ANS balance has thus far been evaluated by each individual HRV parameter calculated for a single 5 min HRV segment, leading to the dynamic activity of the ANS within the same period being ignored. Therefore, to resolve this problem, HRV parameters for ultra-short-term segments that are short enough to reflect a sudden motion artifact must be analyzed. The aim of the present study was to evaluate the effects of a motion artifact on the variation in HRV parameters to provide detailed information on ANS activity. The 121 ultra-short-term HRV segments were created by moving a 1-min window forward by a time shift interval of 2 s for the entire 5 min HRV segment. The ratios of Ln LF to Ln HF in these ultra-short-term segments and a single 5 min segment with a motion artifact were 0.89 and 1.06, respectively, while those in a motion artifact-free HRV segment were 0.75 and 0.93, respectively. This variation test for a short-term motion artifact and motion artifact-free HRV dataset was found to affect the SDNN (7.73 and 2.68), SD2 (11.44 and 4.42), TINN (40.33 and 9.92), and Ln HF (0.37 and 0.13) the most in terms of the standard deviation, respectively. Taken together, the mean HRV parameters of many ultra-short-term segments might play an important role in evaluating dynamic ANS activities within a short-term segment, avoiding the false conclusions made by the traditional HRV analysis.

***Keywords* : Autonomic nervous system, heart rate variability, parasympathetic nervous branch, sympathetic nervous branch**

I. INTRODUCTION

Heart rate variability (HRV) has increasingly become a good indicator for the assessment of autonomic nervous system (ANS) imbalances, which result in psychological and cardiovascular diseases in various clinical fields [1]-[3]. As HRV is a measure of the variation in time between two predictable consecutive normal-to-normal heartbeats (NN interval), HRV technology has recently been applied to wearable or mobile devices [4]-[6].

Methods that obtain the NN intervals for HRV recordings include electrocardiogram (ECG) and photoplethysmogram (PPG) measurements. These two measurements are widely accepted as

sufficient for obtaining an accurate NN interval for HRV analysis, but the PPG-type measurement has been preferred because it

imposes a small burden on the subject compared to the ECG-type measurement, which requires an attachment of at least two electrodes to the body [7]. However, both have shortcomings in that both measurements are highly susceptible to body movement or external stimuli, but of the two an ECG is known to be less affected by the ambient environment than the PPG based on optical technology. For the HRV recording regardless of measurement types, a motion artifact must be taken into consideration. A motion artifact is defined as representing all events that can distort a normal NN interval, either body movements (including abrupt deep breathing, coughing, and talking) or any external stimuli. To improve the reliability of HRV results, many studies have attempted to develop advanced algorithms to detect or remove any kind of motion artifact [8]-[10]. However, the complete removal of a motion artifact seems to be impossible at present [11]-[12]. These facts suggest that any motion artifacts cannot help but be essentially included in an HRV recording when measuring for 5 min even under strict environmental control of the internal or external factors. On the other hand, a motion artifact may include important information related to the ANS. HRV can entirely reflect the capacity of a subject's heart to respond to a variety of physiological environmental stimuli by ANS activity for a motion artifact-free HRV dataset [13]. In contrast, the relaxation response that activates the parasympathetic nervous system can be miscalculated by even a very short abdominal belly breath from the HRV parameters. A dynamic activity of the ANS for a 5 min epoch could experience repeated changes between parasympathetic and sympathetic nerve activities, which correspond to the high frequency (HF) and low frequency (LF) bands of the HRV parameters, respectively. In a conventional analysis, the assessment of the ANS balance is performed from the HRV parameters for a single 5 min HRV segment, which will result in a failure to reflect the dynamic performance within the same period.

Manuscript received on March 15, 2020.
Revised Manuscript received on March 24, 2020.
Manuscript published on March 30, 2020.
* Correspondence Author
Jse Mok Ahn*, School of Software, Hallym University, Chuncheon-si, Gangwon-do, South Korea. Email: ajm@hallym.ac.kr
Jeom Keun Kim, School of Software, Hallym University, Chuncheon-si, Gangwon-do, South Korea. Email: jkim@hallym.ac.kr

The necessities of the HRV parameters that reflect a dynamic ANS balance are growing.

Therefore, in this study, to provide detailed information in connection with the ANS activity in an ultra-short period, many ultra-short-term segments were created by moving 1-min window forward by a time shift interval of 2 s for the entire 5 min HRV dataset. This study aimed to improve the reliability of HRV analysis by taking a motion artifact into consideration, which causes changes in the HRV parameters. We evaluated the effect of a motion artifact on variations in the HRV parameters obtained from 121 ultra-short-term HRV segments. This variation test for a short-term motion artifact was found to affect the SDNN, SD2, TINN, and Ln HF the most, and it especially caused larger fluctuations in the nonlinear parameters.

II. HRV PARAMETERS

HRV analysis extracts HRV parameters to identify the autonomic influences of the psychological and physical status on the variation in the NN interval between two successive heartbeats. The HRV parameters are mainly categorized into three domains: frequency-, time-, and geometric domains. The geometric domain is related to nonlinear parameters such as TINN, ApEn, SD1, and SD2 as listed in Table I. A Poincare plot analysis is carried out to show the degree of complexity of the NN intervals. Three parameters are obtained from the shape of the Poincare chart: SD1, SD2, and SD2/SD1. SD1 and SD2 represent the parameters of the instantaneous recording and long-term recording, respectively, respectively. The relationship of both (SD2/SD1) shows the ratio between the short- and long-term variations in the NN intervals [13]-[15]. SD1 and SD2 are calculated with the following equations.

$$SD1 = \sqrt{var(x1)}\,, \qquad x1 = \frac{NN(n+1)-NN(n)}{\sqrt{2}} \tag{1}$$

$$SD2 = \sqrt{var(x2)}\,, x2 = \frac{NN(n+1)+NN(n)}{\sqrt{2}} \tag{2}$$

ApEn is a statistic that can quantify the regularity and complexity of a stationary signal for a number of data points [16]. Its calculation equations are complex and time-consuming, as follows.

$$\mathrm{ApEn(m,r)} = \pi^{m}(r) - \pi^{m+1}(r) \tag{3}$$

$$\pi^{m}(r) = \frac{1}{N-m+1}\sum_{i=1}^{N-m+1} \log[C_i^m(r)] \tag{4}$$

$$C_i^m = \frac{B_i(r)}{(N-m+1)} \tag{5}$$

$$B_i(r) = d[x(i),x(j)] \le r \tag{6}$$

$$d[x(i),x(j)] = \max_{k=1,2,??m}(|u(i+k-1) - u(j+k-1)) \tag{7}$$

For the time domain parameters, the SDNN estimates short cycle lengths in the HRV dataset. The SDNN has been correlated with left ventricular dysfunction, resulting in an increased risk for sudden cardiac death [15]. The RMSSD estimates the fast NN interval variations in the HRV dataset. The SDSD represents short-term variability in assessing the activity of the parasympathetic nerve. The mathematical equations for the SDNN, RMSSD, and SDSD are as follows:

$$SDNN=\sqrt{\frac{\sum_{n=1}^{N-1}(NN_n-\overline{NN})^2}{N-1}} \tag{8}$$

$$RMSSD=\sqrt{\frac{1}{N-1}\sum_{1}^{N-1}[NN_n - NN_{n-1}]^2} \tag{9}$$

$$SDSD=\sqrt{\frac{\sum(NN_{diff}-\overline{NN_{diff}})^2}{N-1}} \tag{10}$$

where $NN_{diff}=NN_n-NN_{n-1}$.

$$CVAA\% = SDNN/\text{mean NN intervals} *100 \tag{11}$$

For frequency domain analysis, three parameters are calculated in the following equations (12)-(14) by the fast Fourier transform (FT): very low frequency (VLF), low frequency (LF), and high frequency (HF). In general, the power spectrum of the VLF band increases at a steady rate throughout the night, and peaks shortly before an individual awakens [16]. The clinical explanation of the VLF band is less clearly defined than that of the LF and HF bands for a short-term HRV segment, but the VLF power has been reported to be related to thermoregulation, the renin-angiotensin system, and other hormonal factors [17]. The LF band is the LF power that reflects both sympathetic and parasympathetic activities but is that in which the sympathetic nerve has dominance over the parasympathetic nerve. The HF band is the HF power that induces parasympathetic activity as the major contributor. The frequency domain parameters of Ln HF, Ln LF and Ln VLF were calculated in real time by using the following equations [18]-[19].

$$\text{Ln HF}=ln\int_a^b |X[k]^2|dk \tag{12}$$

$$\text{Ln LF}=ln\int_c^d |X[k]^2|dk \tag{13}$$

$$\text{Ln VLF}=ln\int_e^f |X[k]^2|dk \tag{14}$$

where the LF band is the activity between a=0.04 and b=0.15 Hz, the HF band is the activity between c=0.15 and d=0.1 Hz, and the VLF band is the activity between e=0.0033 and f=0.04 Hz. The power spectrum, X[k] was calculated as follows.

$$X[k] = \sum_0^{N-1} w[n] * x[n] e^{\frac{-2i\pi kn}{N}} \tag{15}$$

where w[n] is a Hanning widow used to minimize the spectral leakage.

Table- I: Heart rate variability parameters.

TP	ms^2	Area under the entire power spectral curve, VLF+LF+HF
Ln VLF	ms^2	Natural logarithmic value of very low frequency power, bands of 0.0033-0.04 Hz
Ln LF	ms^2	Natural logarithmic value of low frequency power, bands of 0.04-0.15 Hz
Ln HF	ms^2	Natural logarithmic value of high frequency power, bands of 0.15-0.40 Hz
LF norm	nu	Normalized low frequency power
HF norm	nu	Normalized high frequency power
Ln LF/Ln HF		Ratio of the low to high frequency power
SDNN	ms	The standard deviation of all NN intervals
RMSSD	ms	The square root of the mean of the sum of the squares of differences between adjacent NN intervals
SDSD	ms	The standard deviation of the differences between adjacent NN intervals

CVAA	%	Coefficient of variation of the a-a intervals
TINN	ms	Baseline width of the minimum square difference triangular interpolation of the highest peak on the NN interval histogram
ApEn		Approximate entropy
SD1	ms	One standard deviation of the length of the transverse line on the Poincare plot
SD2	ms	Two standard deviation of the length of the longitudinal line on the Poincare plot

III. PROCESSING SCHEMES

Two 5 min HRV recordings using a commercial pulse analyzer with a finger-type sensor of a photoplethysmogram (PPG), TAS9VIEW (CANOPY9 RSA, IEMBIO Co. Ltd.,

Chuncheon-si, South Korea) were obtained. One was obtained without any motion artifact, while the other was obtained with a short-term motion artifact due to a short-term deep breathing that took place in the initial stage of the entire length as shown in Fig. 1. The processing scheme was designed to investigate the effects of a motion artifact on the HRV parameters in the time, frequency, and geometric domains. The 121 1-min segments were created by shifting the 1-min window forward by a time shift interval of 2 s for the entire 5 min HRV dataset using the research mode provided by TAS9VIEW. The research mode provides a powerful function of various options, such as a full-time range and time shift, which can select a random duration of the HRV dataset and time shift intervals from 2 s to 900 s, respectively. It was not important in this study to check the participant's health status because the purpose of the study was to investigate the HRV parameters that can affect a motion artifact the most.

IV. RESULTS AND DISCUSSION

Fig. 2 shows the trajectory of all the LF and HF parameters calculated by moving a 1-min window forward by a time shift interval of 2 s for a 5 min segment. The differences between the maximum LF and minimum LF for a motion artifact segment and motion artifact-free segment were 5.56 and 2.81 ms^2, respectively, while those between the HFs were 1.68 and 0.57 ms^2, respectively, as listed in Table II and III. The difference rate between the LFs doubled in a motion artifact segment, compared to the difference rate in a motion artifact-free segment, while that between the HFs approximately tripled. This result means that a motion artifact influenced the parasympathetic nervous branch more than the sympathetic nervous branch, even though it implied more sympathetic activity than parasympathetic activity. Additionally, the standard deviations of the LFs and HFs for motion artifact and motion artifact-free segments were 0.64 and 0.13 ms, and were 1.35 and 0.37 ms, respectively. One of the HRV parameters with a large difference between the motion artifact and motion artifact-free segments was SD2 in terms of the standard deviation, which was 2.58 higher in a motion artifact segment than in a motion artifact-free segment, as shown in Fig. 3. However, there was no significant difference between the means of SD2 for the two HRV segments. Fig. 4 shows a Poincare plot for two HRV datasets: without a motion artifact (top figure) and with a motion artifact (bottom figure). For the motion artifact segment, SD1 resulted much less variation than did SD2, with 1.33 and 11.44 ms in the standard deviation, respectively. The results suggested that SD2 was highly linked to the parasympathetic nervous system, with SD1 reflecting the sympathetic nervous system. The rate of SD2 to SD1 was three times higher in the motion artifact segment than in the motion artifact-free segment. One of the other HRV parameters that can differentiate a motion artifact from a non-motion artifact in the HRV segment is the SDNN, the mean values of which are 18.35 and 21.81 ms, respectively. Although the value of the SDNN for a motion artifact segment was approximately 15.8 % lower than that for a motion artifact-free segment, their standard deviations of the SDNNs were 7.73 and 2.68 ms, respectively. It is understood that the SDNN is highly related to the parasympathetic nervous system. Meanwhile, the RMSSD has been used as the parameter for assessing parasympathetic activity, but there was a moderate difference between the two HRV segments. The standard deviation of the RMSSD for a motion artifact segment was only 1.86 ms, compared to 7.73 ms in the SDNN. For the assessment of parasympathetic activity using the LF value, the SDNN is recommended rather than the RMSSD. The largest difference between the standard deviations was a TINN with a value that is four times higher in a motion artifact segment (40.33 ms) than in a motion artifact-free segment (9.92 ms), while the smallest difference occurred for the ApEn. The ApEn parameter for the HRV analysis needs to be more carefully considered in evaluating physical and mental status in clinical applications, before investigating its clinical meaning thoroughly.

Table- II: Major HRV parameters for a motion artifact-free HRV dataset obtained by considering 121 1-min segments and a single 5 min segment.

	1 min by 2 s		5 min
	Mean (n=121)	STD	Mean
Mean NN	911	-	915
SDNN	21.81	2.68	24.57
RMSSD	25.20	1.03	25.41
pNN50 %	1.32	1.34	1.52
ApEn	0.3583	0.0846	1.0416
SD1	17.95	0.73	18.00
SD2	25.23	4.42	29.71
Min. SD2	19.47	-	-
Max. SD2	37.07	-	-
Diff. SD2	17.60	-	-
SD2/SD1	1.40	0.23	1.65
Ln sArea	7.25	0.19	7.43
SDSD	25.00	1.02	25.37
TINN	93.69	9.92	122.00
CVAA %	2.40	0.99	2.85
SDANN	6.55	-	-

SDNN index	21.81	-	-
Ln TP	5.63	0.08	5.61
Ln VLF	4.94	0.03	4.77
Ln LF	3.47	0.64	4.17
Ln HF	4.60	0.13	4.50
Ln LF/Ln HF	0.75		0.93
Min. Ln LF	1.73	-	-
Max. Ln LF	5.54	-	-
Diff. Ln LF	2.81	-	-
Min. Ln HF	4.33	-	-
Max. Ln HF	4.9	-	-
Diff. Ln HF	0.57	-	-

Table- III: Major HRV parameters for a normal HRV dataset with a motion artifact obtained by considering 121 1-min segments and a single 5 min segment.

	1 min by 2 s		5 min
	Mean (n=121)	STD	Mean
Mean NN	764	-	767
SDNN	18.35	7.73	21.83
RMSSD	14.78	1.86	15.26
pNN50 %	0.37	0.90	0.51
ApEn	0.5068	0.0998	1.2776
SD1	10.52	1.33	10.81
SD2	23.65	11.44	28.98
Min. SD2	12.36	-	-
Max. SD2	49.73	-	-
Diff. SD2	37.37	-	-
SD2/SD1	2.17	0.74	2.68
Ln sArea	6.56	0.52	6.89
SDSD	14.68	1.85	15.24
TINN	82.55	40.33	162.00
CVAA %	2.39	0.29	2.68
SDANN	5.63	-	-
SDNN index	18.35	-	-
Ln TP	5.26	0.54	5.42
Ln VLF	4.59	0.04	5.00
Ln LF	3.33	1.35	3.74
Ln HF	3.74	0.37	3.54
Ln LF/Ln HF	0.89		1.06
Min. Ln LF	1.17	-	-
Max. Ln LF	6.73	-	-
Diff. Ln LF	5.56	-	-
Min. Ln HF	3.25	-	-
Max. Ln HF	4.93	-	-
Diff. Ln HF	1.68	-	-

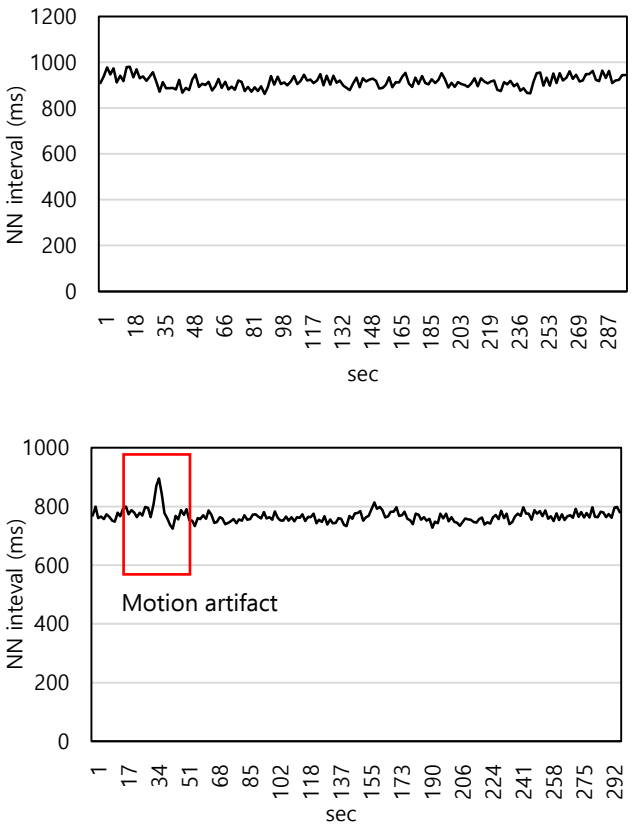

Fig. 1. Two tachograms measured for a 5 min HRV dataset: (top) a motion artifact-free tachogram and (bottom) a tachogram with a motion artifact.

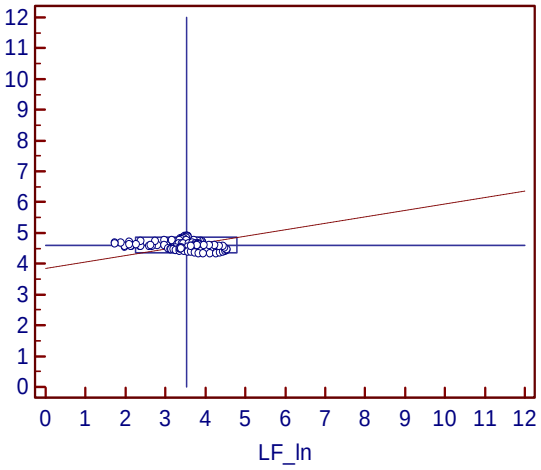

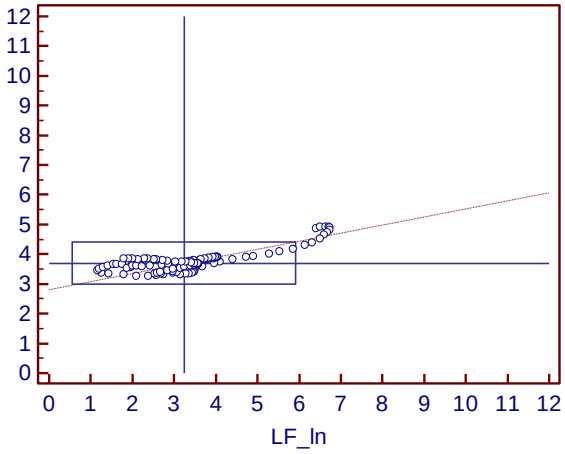

Fig. 2. A trajectory of the ANS balance in terms of the LF and HF: (top) motion-free and (bottom) motion artifact projectiles.

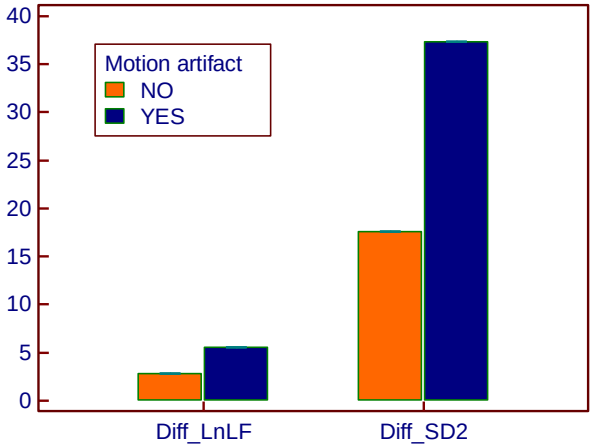

Fig. 3. A comparison between the motion artifact-free and motion artifact HRV datasets in terms of the Ln LF and SD2.

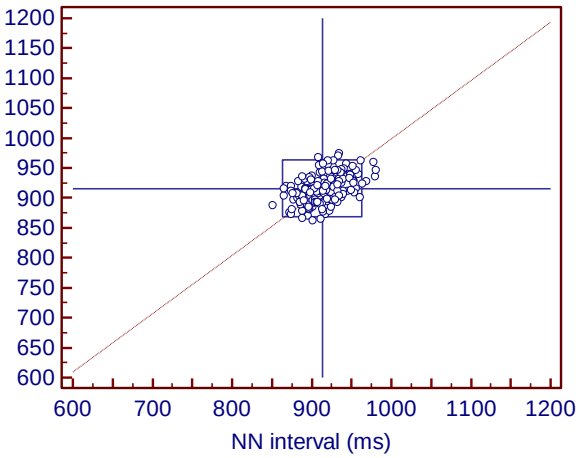

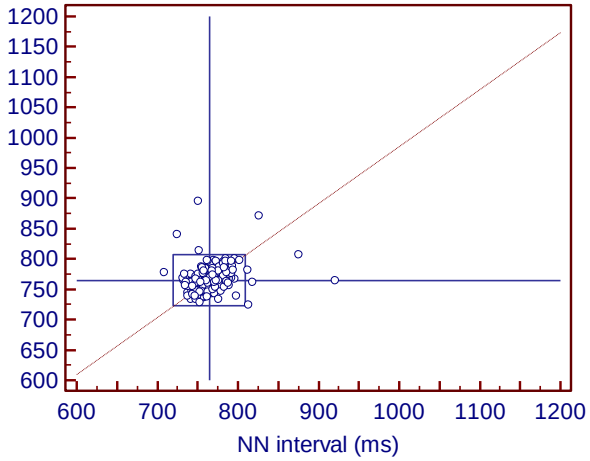

Fig. 4. Poincare plot for two tachograms without and with motion artifacts (top and bottom plots, respectively).

V. CONCLUSION

The effects of a motion artifact on the HRV parameters for HRV analysis were thoroughly investigated by using the results obtained from 121 segments, which were created by moving a 1-min window segment forward by a time shift interval of 2 s for a 5 min HRV segment. The HRV results for a 5 min segment provided only a single parameter at a time, such as the values of the LF and HF, which have been used as inputs for clinical assessments. However, continuing changes in parasympathetic and sympathetic nervous activities, which might take place within a short-term period have not been understood. These changes indicate that if a motion artifact is generated due to a real change in the ANS and not a body movement, the HRV analysis may be different. In this study, for example, the result of a 5 min HRV segment with a motion artifact showed sympathetic nerve dominance, but time shift analysis with many 1-min windows showed a greater amount of parasympathetic nerve activity more than that of sympathetic nerve activity. The balance between parasympathetic and sympathetic nerve activities was reflected by a large change in the SDNN, SD2, SD2/SD1, TINN, and Ln HF values in terms of the standard deviation, and by a small change in the RMSSD, SD1, SDSD, and Ln LF values. If a motion artifact appeared due to a body movement or other interference, the reliability of the HRV results could be estimated to a certain extent by evaluating changes in the HRV parameters mentioned above. Taken together, many ultra-short-term segments with a certain time shift interval for different window sizes might play a critical role in assessing dynamic activities within a short-term segment to avoid obtaining false results from conventional analysis.

ACKNOWLEDGMENT

This work was supported by the Hallym University Research Fund (HRF-202003-019).

REFERENCES

1. A. Malliani, "Cardiovascular neural regulation explored in the frequency domain," *Circulation*, 1991, vol. 84, pp. 482-492.
2. S. Evans, L.C. Seidman, J.C.I. Tsao, K.C. Lung, L.K. Zeltzer, B.D. Naliboff, "Heart rate variability as a biomarker for autonomic nervous system response differences between children with chronic pain and healthy control children," *Journal of Pain Research*, 2013, vol. 6, pp. 449-457.
3. P.J. Schwartz, M.T. La Rovere, E. Vanoli, "Autonomic nervous system and sudden cardiac death. experimental basis and clinical observations for post-myocardial infarction risk stratification," *Circulation*, 1992, vol. 85, no. 1, pp.177-191.
4. L. Wang, B.P. Lo, G.Z. Yang, "Multichannel reflective PPG earpiece sensor with passive motion cancellation," *IEEE Transaction on Biomedical Circuits and Systems*, 2007, vol. 1, no. 4, pp. 235-241.
5. M.Z. Poh, N.C. Swenson, R.W. Picard, "Motion-tolerant magnetic earring sensor and wireless earpiece for wearable photoplethysmography," *IEEE Transactions on Information Technology in Biomedicine*, 2010, vol. 14, no. 3, pp. 786-794.
6. J.A. Healey, R.W. Picard, "Detecting stress during real-world driving tasks using physiological sensors," *IEEE Transactions on Intelligent Transportation Systems*, 2005, vol. 6, no. 2, pp. 156-166.
7. J.N. Froning, M.D. Olson, V.F. Froelicher, "Problems and limitations of ECG baseline estimation and removal using a cubic spline technique during exercise ECG testing: Recommendations for proper implementation," *Journal of Electrocardiology*, 1988, vol. 21, Supplement, pp. S149-S157.
8. David Pollreisz, Nima TaheriNejad, "Detection and removal of motion artifacts in PPG signals," *Mobile Networks and Applications*, 2019, vol. 8, pp. 1-11.
9. C.C. Wu, I.W. Chen, W.C. Fang, "An implementation of motion artifacts elimination for PPG signal processing based on recursive least squares adaptive filter," *In: 2017 IEEE Biomedical circuits and Systems conference (BioCAS)*, 2017, pp. 1-4.
10. W.J. Lin, H.P. Ma, "A physiological information extraction method based on wearable PPG sensors with motion artifact removal," *In: 2016 IEEE International conference on communication (ICC)*, 2016, pp. 1-6.
11. K.A. Reddy, B. George, V.J. Kumar, "Use of Fourier series analysis for motion artifact reduction and data compression of photoplethysmographic signals," *IEEE Transactions on Instrumentation and Measurement*, 2009, vol. 58, no. 5, pp. 1706-1711.
12. R. Krishnan, B. Natarajan, S. Warren, "Two-stage approach for detection and reduction of motion artifacts in photoplethysmographic data," *IEEE Transactions on Biomedical Engineering*, 2010, vol. 57, no. 8, pp. 1867-1876.
13. A.U Rajendra, J.K. Paul, N. Kannathal, C.M. Lim, J.S. Suri, "Heart rate variability: a review," Med Bio Eng Comput, 2006, vol. 44, no. 12, pp. 1031-1051.
14. F.X. Gamelin, S. Berthoin, L. Bosquet, "Validity of the polar S810 heart rate monitor to measure R-R intervals at rest," Med Sci Sports Exerc, 2006, vol. 38, no. 5, pp. 887-893.
15. De Vito G, S.D. Galloway, M.A. Nimmo, P. Maas, J.J. McMurray, "Effects of central sympathetic inhibition on heart rate variability during steady-state exercise in healthy humans," Clin Physiol Funct Imaging, 2002, vol. 22, no. 1, pp. 32-38.
16. Task Force of the European Society of Cardiology and the North American Society of Pacing and Electrophysiology, "Heart Rate Variability standards of measurement, physiological interpretation, and clinical use," *Circulation*, 1996, vol. 93, pp. 1043-1065.
17. S. Cerutti, A.M. Bianchi, L.T. Mainardi, "Spectral Analysis of the Heart Rate Variability Signal," *In: Malik, M. and Camm, A.J., Heart Rate Variability. Armonk NY: Futura Publishing Company, Inc.*, 1995, pp. 63-74.
18. J.K. Kim, J.M. Ahn, "Effects of a spectral window on frequency domain HRV parameters," *Advances in Computer Communication and Computational Sciences*, 2019, vol. 924, pp. 697-710.
19. J.M. Ahn, J.K. Kim, "Evaluation of heart rate variability indices during postural changes," International Journal of Scientific and Technology Research, 2019, vol. 8, no. 11, pp. 1200-1205.

AUTHORS PROFILE

Jae Mok Ahn received the B.E. degree in electronics engineering and Ph.D. degree in biomedical engineering from Seoul National University, Seoul, South Korea. Since Spring 1998, he has been a faculty member at the department of electronics engineering, school of software, Hallym University. He is currently engaged in research on improving healthcare system, bio-signal analysis, heart rate variability, and acceleration plethysmogram. He has developed a pulse analyzer that provides the judgment of a vascular status and activity of autonomic nervous system for healthcare system. He is a member of the Korean Society for Biomedical Engineering.

Jeom Keun Kim received the B.E. degree in control and instrumentation engineering and Ph.D. degree in mechatronics from Seoul National University, Seoul, South Korea. Since Spring 1994, he has been a faculty member at the department of electronics engineering, school of software, Hallym University. His research interests include motor control, smart farm control system, spirometer, healthcare communication, and signal processing techniques. In particular, he has developed a smart spirometry that gives information related to lung capacity, with a newly detection system of slight changes in air pressure flowing in and out through a mouthpiece being introduced.